

UNIVERSITY OF  
CALIFORNIA

*Ernest O. Lawrence*

*Radiation  
Laboratory*

ION DENSITY MEASUREMENTS IN A DECAYING  
HYDROGEN PLASMA

TWO-WEEK LOAN COPY

*This is a Library Circulating Copy  
which may be borrowed for two weeks.  
For a personal retention copy, call  
Tech. Info. Division, Ext. 5545*

## **DISCLAIMER**

This document was prepared as an account of work sponsored by the United States Government. While this document is believed to contain correct information, neither the United States Government nor any agency thereof, nor the Regents of the University of California, nor any of their employees, makes any warranty, express or implied, or assumes any legal responsibility for the accuracy, completeness, or usefulness of any information, apparatus, product, or process disclosed, or represents that its use would not infringe privately owned rights. Reference herein to any specific commercial product, process, or service by its trade name, trademark, manufacturer, or otherwise, does not necessarily constitute or imply its endorsement, recommendation, or favoring by the United States Government or any agency thereof, or the Regents of the University of California. The views and opinions of authors expressed herein do not necessarily state or reflect those of the United States Government or any agency thereof or the Regents of the University of California.

UCRL-9509  
UC-20 Controlled Thermo-  
nuclear Process  
TID-4500 (16th Ed.)

UNIVERSITY OF CALIFORNIA

Lawrence Radiation Laboratory  
Berkeley, California

Contract No. W-7405-eng-48

ION DENSITY MEASUREMENTS IN A DECAYING HYDROGEN PLASMA

William S. Cooper III, Alan W. DeSilva, and John M. Wilcox

March 1, 1961

Printed in USA. Price 75 cents. Available from the  
Office of Technical Services  
U. S. Department of Commerce  
Washington 25, D.C.

## ION DENSITY MEASUREMENTS IN A DECAYING HYDROGEN PLASMA

William S. Cooper III, Alan W. DeSilva, and John M. Wilcox

Lawrence Radiation Laboratory  
University of California  
Berkeley, California

March 1, 1961

## ABSTRACT

A hydrogen plasma was prepared for Alfvén wave experiments and was allowed to decay. The shapes of the Stark broadened line profiles of the first three members of the Balmer series,  $H_{\alpha}$ ,  $H_{\beta}$ , and  $H_{\gamma}$ , were measured as functions of time and were matched with theoretical line profiles calculated by Griem, Kolb, and Shen to obtain the ion density as a function of time. In the 300  $\mu$ sec during which the line profiles were observed the ion density decayed from  $5.0 \times 10^{15} \text{ cm}^{-3}$ , to  $1.5 \times 10^{15} \text{ cm}^{-3}$ , and extrapolated back to  $5.5 \times 10^{15}$  to  $7.1 \times 10^{15} \text{ cm}^{-3}$  at the time the discharge current was terminated, corresponding to 85 to 100% ionization of the hydrogen initially in the tube. A nearly pure Balmer spectrum, merging with the continuum after nine lines, was observed. The observed depression of the series limit indicated a time-averaged ion density of about  $3 \times 10^{15} \text{ cm}^{-3}$ , in good agreement with the measurements from the profiles of the three individual lines. The observed velocity of Alfvén waves in the plasma yielded a value for the ion density that was also in good agreement with these spectroscopically determined values. The temperature was estimated to be about 10,000  $^{\circ}$ K. The plasma probably decays by a volume recombination process in the manner described by D'Angelo.

## ION DENSITY MEASUREMENTS IN A DECAYING HYDROGEN PLASMA

William S. Cooper III, Alan W. DeSilva, and John M. Wilcox

Lawrence Radiation Laboratory  
University of California  
Berkeley, California

March 1, 1961

Experimental work previously reported has verified the existence of torsional hydromagnetic (Alfvén) waves.<sup>1,2,3,4</sup> To verify the theoretical expression for the velocity of these hydromagnetic waves,

$$V = B / \sqrt{4\pi\rho},$$

it is necessary to determine  $\rho$ , the mass density of the particles participating in the wave motion. In a fully ionized plasma, this corresponds to the mass density of the ions in the plasma. If the species of ion is known, it is sufficient to measure the ion particle density,  $N_i$ . As the wave experiments are generally performed in a decaying plasma, it is desirable to determine the ion density as a function of time. The time dependence of the ion density in a decaying plasma is, in itself, of considerable interest, as it may yield information about the various recombination and diffusion processes that take place.

We determined the ion density of a decaying hydrogen plasma as a function of time by observing the time dependence of the Stark-broadened profiles of the first three spectral lines of the hydrogen Balmer series,  $H_\alpha$ ,  $H_\beta$ , and  $H_\gamma$ . The half width of these spectral lines is roughly proportional<sup>a</sup> to  $N_i^{2/3}$ .

## THEORY

The lines are broadened by the familiar Stark effect, in which the energy levels of a radiating atom located in the plasma are perturbed by the Coulomb electric fields of neighboring ions and electrons. This is a statistical effect, depending on the positions of the near-by ions and electrons, and, if suitable statistical averages are taken over all possible configurations, the resulting emission line profile can be predicted. In the case of hydrogen and hydrogenlike atoms, which exhibit a large first-order Stark effect, the net result is a broadening of the line. This broadening of the line profile can then be used to determine experimentally the ion density in the plasma.

J. Holtsmark published the first theoretical treatment of this problem in 1919.<sup>5</sup> He considered the Stark broadening of the hydrogen lines due to the Coulomb fields of slowly moving ions near the radiating atom.

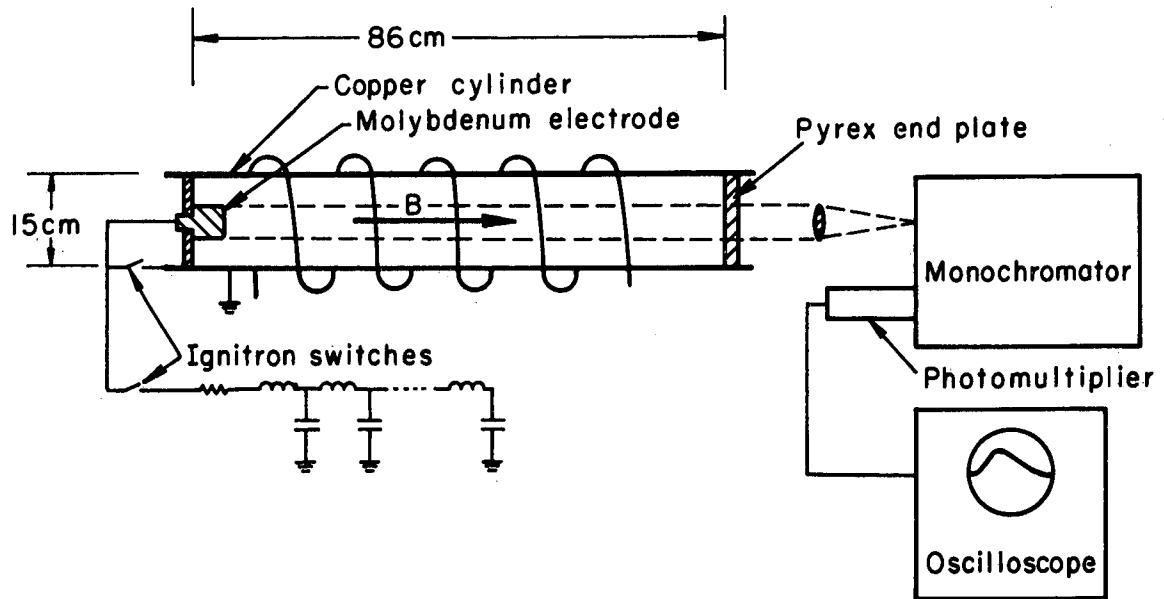
A much more comprehensive treatment of this problem was carried out by H. R. Griem, A. C. Kolb, and K. Y. Shen in 1959.<sup>6</sup> They considered the effects of the local fields of both ions and electrons, the effect of electron collisions with the radiating atoms (which is to broaden the line profiles still more and also to make the shape of the line profiles somewhat temperature-dependent), and also the effect of electron shielding and ion-ion correlation on the ion field-strength distribution function. They estimate that an accuracy of about 10% may be expected in their theoretical curves. The second-order Stark effect was not considered. This effect would make the resulting line profiles asymmetric, but it can be shown to be very small at our ion densities. An  $H_{\beta}$  profile determined experimentally by P. Bogen<sup>7</sup> agrees with Griem, Kolb,<sup>6</sup> and Shen's theoretical profile to within 10% over a range of two orders of magnitude in intensity.

An independent calculation of the theoretical  $H_{\beta}$  profiles by B. Mozer<sup>8</sup> is in excellent agreement both with Griem, Kolb,<sup>6</sup> and Shen's theoretical calculations and with Bogen's experimental work, so that it would appear that their theoretical profiles may be expected to be quite accurate. A thorough review of the various theories of line broadening is given in an article by Margenau and Lewis.<sup>9</sup>

We have assumed Griem, Kolb, and Shen's calculations to be correct, and have used their theoretical line profiles to determine the ion density in the decaying plasma.

## EXPERIMENTAL TECHNIQUES

A schematic diagram of the experiment is shown in Fig. 1. The method of preparing the plasma has been discussed elsewhere,<sup>3,4</sup> and will be only reviewed briefly here. A cylindrical copper tube immersed in a uniform axial magnetic field of 16,000 gauss is filled with hydrogen at a pressure of 100  $\mu$  of Hg. The hydrogen used was 99.9% pure Matheson Co. electrolytic hydrogen, and flowed continuously through the tube during the course of the experiment. A lumped-constant pulse line charged initially to 10,000 volts provides a constant-current pulse of about 10,000 amp. This current, flowing between the molybdenum electrode at one end of the tube and the outer copper wall, drives an ionizing wave somewhat similar to a "switch-on" shock down the tube in about 20  $\mu$ sec under these conditions, leaving behind it a highly ionized plasma, which is spinning because of  $\mathbf{j} \times \mathbf{B}$  forces. If the driving current is allowed to continue to flow after the ionizing wave reaches the far end of the tube, prominent impurity lines due to O, O<sup>+</sup>, Si<sup>+</sup>, Si<sup>++</sup>, and Si<sup>+++</sup> appear in the spectrum of the discharge, coming, no doubt, from the pyrex end plate which seals that end of the tube. To prevent the influx of these impurities into the plasma, when the ionizing wave reaches the end of the tube we "crowbar" (short-circuit) the pulse line and abruptly terminate the flow of current into the plasma. The spinning plasma, now shorted, comes to rest in about 15  $\mu$ sec a time determined by external circuit parameters. About this time the plasma starts to decay, either by some volume-recombination process or by diffusion to the wall and recombination there, or both. It was during this time that the ion density measurements were made.



MU - 21659

Fig. 1. Schematic diagram of the equipment.

Light from a column of plasma 5 cm in diameter and concentric with the axis of the tube was carefully focused on the entrance slit of a Jarrell-Ash Model 82-000 monochromator. The output of the DuMont 6292 photomultiplier used with the monochromator was displayed on a Tektronix Type 551 oscilloscope. In taking the data, the monochromator was first set at a given point on the profile of the line, say 10 Å from the center of the line, and the oscilloscope trace photographically recorded. As there was some fluctuation in intensity from shot to shot (the rms fluctuation was about 20%) several shots, usually six, were taken and the results averaged, giving the average intensity as a function of time at this particular point on the line profile. The monochromator was then adjusted to a different wave length and the process repeated. In this way the line profile was scanned. Cross plots then gave the shape of the line profile as a function of time.

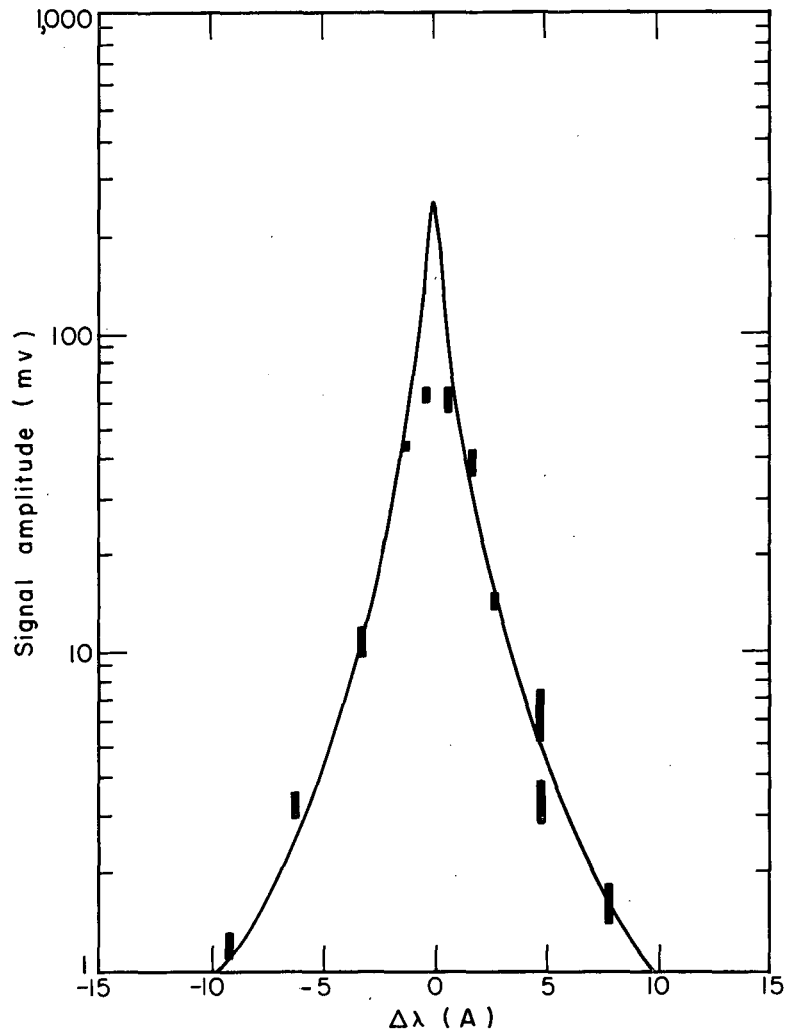
A theoretical profile was fitted to the experimental data in the following manner: a family of theoretical profiles for different ion densities was plotted on semilog graph paper, then the experimental points, also plotted on semilog graph paper, were overlaid and the two displaced vertically with respect to each other until the best match was obtained.

### EXPERIMENTAL RESULTS

Figures 2, 3, and 4 show typical experimentally determined line profiles; they are the profiles of  $H_{\alpha}$ ,  $H_{\beta}$ , and  $H_{\gamma}$  at 50  $\mu$ sec after the discharge was initiated, or 31  $\mu$ sec after the ionizing wave reached the end of the tube and the driving current was crowbarred. The experimental data have all been fitted with theoretical profiles in the manner described above, and the best fit in each case was obtained by assuming an ion density of  $5.0 \times 10^{15} \text{ cm}^{-3}$ . Line profiles later in time were generally similar to those shown in Figs. 2, 3, and 4, except that they were narrower, and were fitted to theoretical profiles in the same way. The sizes of the rectangles about the experimental points in Figs. 2, 3, and 4 indicate the experimental errors—the standard deviation of the mean in the intensity, and the resolving power of the monochromator and setting errors in  $\Delta\lambda$ . Note that it is possible to fit all three lines simultaneously with theoretical profiles calculated for the same ion density,  $5.0 \times 10^{15} \text{ cm}^{-3}$ . A temperature of 10,000 °K was assumed.

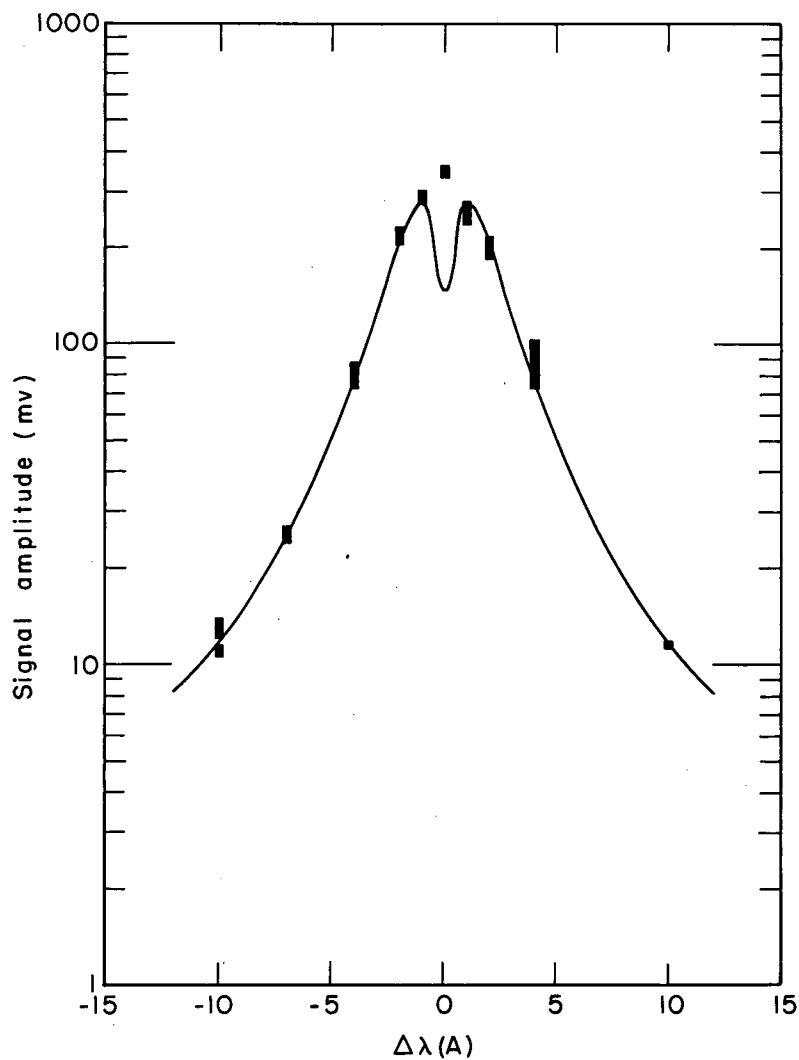
### COMPARISON OF EXPERIMENTAL AND THEORETICAL PROFILES

Agreement of the experimental and theoretical line profiles of  $H_{\alpha}$ , shown in Fig. 2, is not particularly good near the center of the line. This apparent clipping of the peak is probably due to reabsorption of the light within the plasma, which might be expected to become noticeable at these densities. Cowan and Dieke show that the effect of reabsorption in a continuously excited source is essentially a clipping of the peak of the line, without seriously modifying the shape of the wings of the line.<sup>10</sup> Assuming this observed clipping of the peak of  $H_{\alpha}$  to be due to reabsorption, one can estimate the effect of reabsorption on the shape of the rest of the line, and one finds that for  $\Delta\lambda = 4\text{Å}$  the effect is already less than the experimental errors, and is much less out on the wings of the line. One can also estimate the effect of reabsorption on the  $H_{\beta}$  and  $H_{\gamma}$  profiles. The effect on  $H_{\beta}$  would be to reduce the



MU-21662

Fig. 2. H $\alpha$  profile 50  $\mu$ sec after the discharge was initiated. The solid curve is a theoretical profile computed for  $N_i = 5.0 \times 10^{15} \text{ cm}^{-3}$ ,  $T = 10^4 \text{ }^\circ\text{K}$ .



MU-22433

Fig. 3. H $\beta$  profile 50  $\mu$ sec after the discharge was initiated. The solid curve is a theoretical profile computed for  $N_i = 5.0 \times 10^{15} \text{ cm}^{-3}$ ,  $T = 10^4 \text{ }^\circ\text{K}$ .

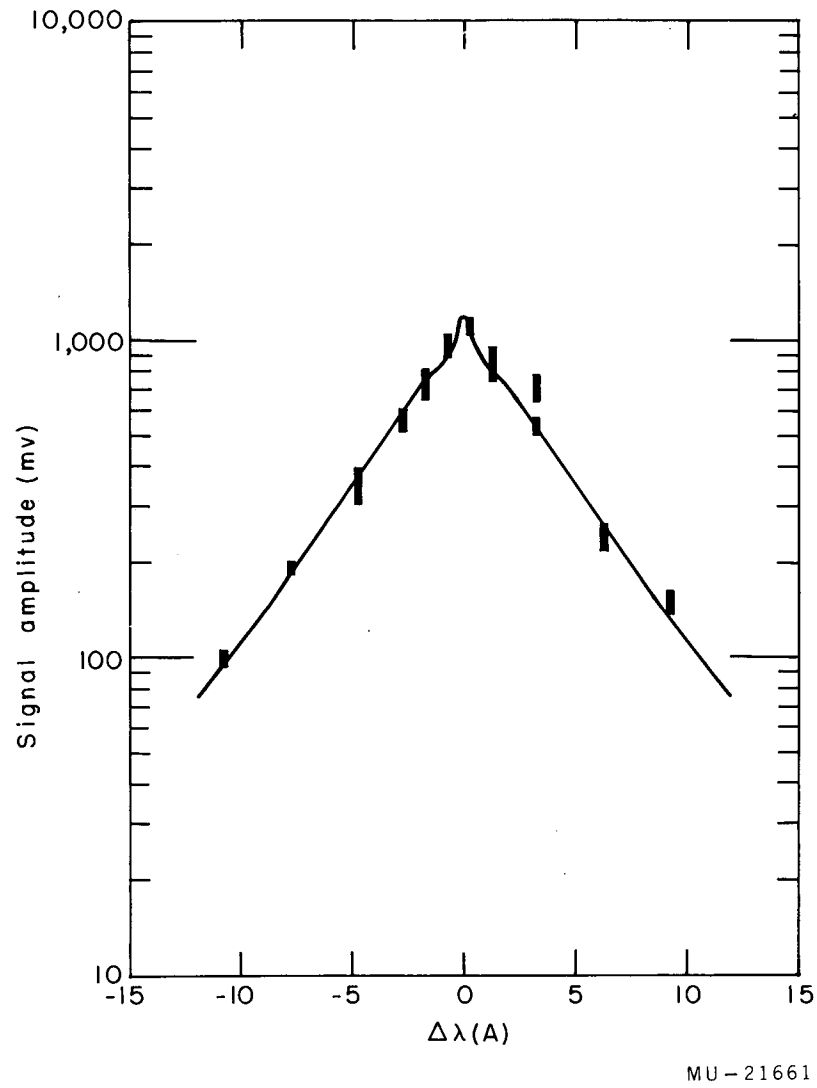


Fig. 4.  $H_{\alpha}$  profile 50  $\mu$ sec after the discharge was initiated. The solid curve is a theoretical profile computed for  $N_i = 5.0 \times 10^{15} \text{ cm}^{-3}$ ,  $T = 10^4 \text{ K}$ .

intensity at the center of the line by about 10%, and elsewhere by much less, and the effect of reabsorption in the case of  $H_{\gamma}$  can be neglected entirely.

The theoretical dip in the center of the  $H_{\beta}$  profile, shown in Fig. 3, was not observed. It may have been filled in by light from a region of the plasma of much lower ion density, such as must be found near the pyrex end plate, or by additional broadening of the two peaks by Zeeman effect or Doppler broadening, both of the order of 0.5 Å. The  $H_{\gamma}$  profile, in Fig. 4, shows good agreement with the theoretical profile everywhere.

### EXPERIMENTAL ERRORS IN DETERMINING ION DENSITIES

A number of effects contribute to experimental errors in determining ion densities by this method. We examine some of these sources of error in detail.

As mentioned earlier, there is considerable variation from shot to shot in the intensity at a given point on the line profile at a given time. It is not yet known whether this variation from shot to shot is caused by variations in the total intensity of the line (a linear scaling of every point on the profile of the line) or by variations in the shape of the line. Because of these shot-to-shot variations it was necessary to take several (usually six) shots at each point on the line profile and average the time dependence, making the taking of data rather tedious. The resulting possible errors in the experimental data limit the precision with which the data may be compared with a theoretical profile. We are currently constructing a multichanneled monochromator, or "polychromator," to enable us to determine the time dependence of a line profile and the ion density, using only a single discharge.

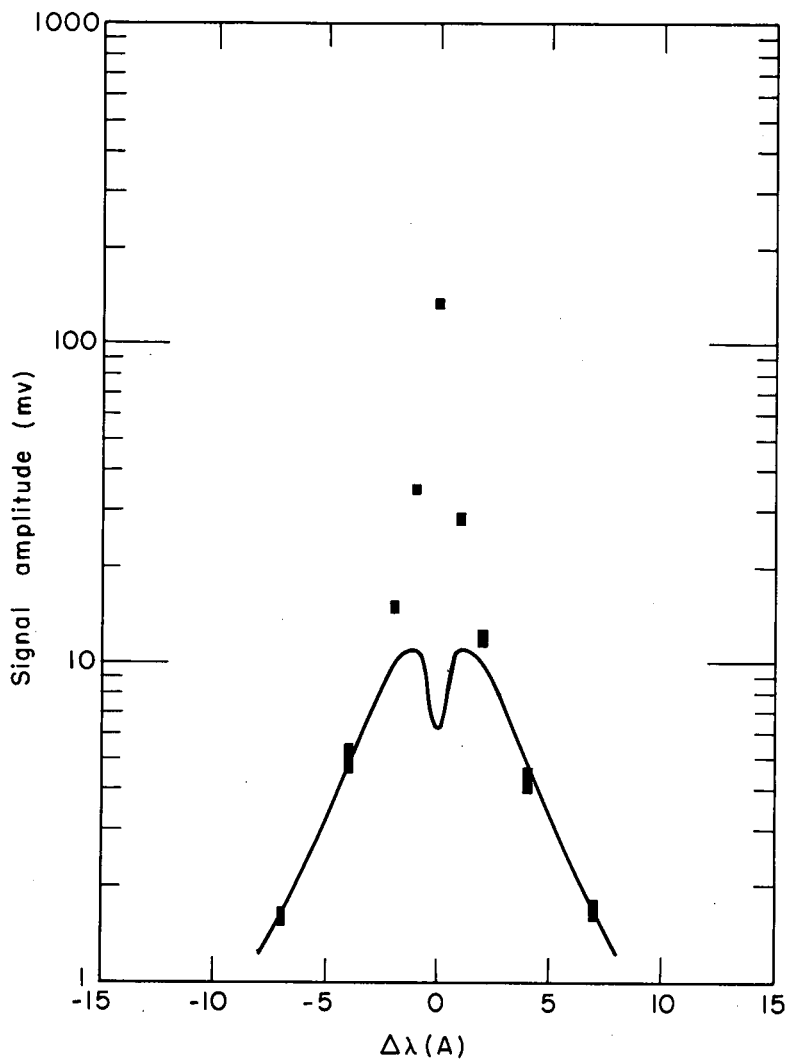
Another possible source of error lies in the spectral response and resolving power of the optical system. The spectral response of the entire optical system was determined by calibration against the almost grey-body spectrum of a hot tungsten filament. This small correction to the shape of the experimentally determined line profiles was always less than 10% over the width of the lines and was neglected. The resolving power of the monochromator, determined experimentally, was 0.22 to 0.59 Å, depending on the widths of entrance and exit slits used, and was much less in all cases than the total widths of the lines, which were observed over a range of some 20 Å.

The long-time response of the photomultiplier circuit used with the monochromator was experimentally determined by observing the response to a 15-msec square light pulse of intensity comparable to that of the light pulse from the discharge. The gain of the photomultiplier did not change by more than 1 or 2% during this pulse, and so was essentially constant during the time of observation of the light pulse from the discharge, which typically lasted about 500  $\mu$ sec. The short-time response was about 10  $\mu$ sec, the RC time constant of a filter at the input of the oscilloscope. This filter greatly improved the precision of measurement of the low-intensity light signals, which were otherwise accompanied by a great deal of high-frequency "grass" (shot noise).

As the experimental profiles were necessarily the result of a large number of individual shots (60 to 70 in all), and several hours were required to take the data, one might expect the usual drifting of amplifier gains, discharge characteristics, etc., that plague experimentalists. To check for long-time drift, one point on the higher-wave-length wing of each line at  $\Delta\lambda \approx 4\text{A}$  was retaken after the entire line was scanned in the direction of decreasing wave length. In the case of the  $H_\beta$  profile (Fig. 3) the points coincided within the experimental errors. In the case of  $H_\alpha$  (Fig. 2) and  $H_\gamma$  (Fig. 4) the points did not overlap but were still in fairly good agreement. The first point taken for  $H_\alpha$  was higher than the second; for  $H_\gamma$  the second point taken was higher. These two profiles were taken simultaneously, by using a second monochromator and a beam splitter not shown in Fig. 1, so that there was at least no drastic change in the characteristics of the discharge during the time required for taking the data.

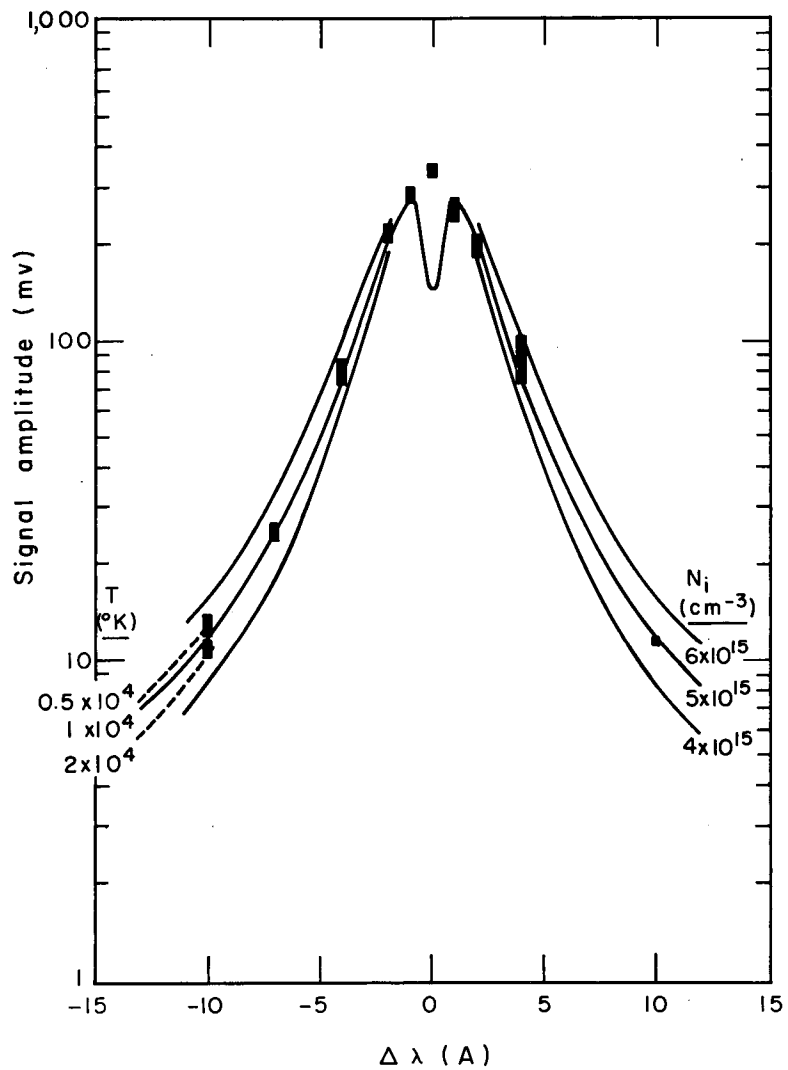
Because of the method of producing the plasma by a type of shock wave, one might expect inhomogeneities in the plasma due either to turbulence behind the ionizing wave or to the necessary mass motion of the plasma along the axis of the tube behind the wave. We must therefore consider the effect of these inhomogeneities, if they exist, on the shapes of the line profiles. A systematic study of possible inhomogeneities would require looking simultaneously at light from different regions of the plasma, and this has not yet been done. We do, however, have evidence of the effect on the line shapes of a strong gradient in ion density. Figure 5 shows an  $H_\beta$  profile 19  $\mu\text{sec}$  after the discharge was initiated, just as the ionizing wave reached the end of the tube and while the ionizing current was still flowing. The solid curve is a profile computed for  $N_1 = 6.4 \times 10^{15} \text{ cm}^{-3}$ ,  $T = 10,000^\circ\text{K}$ , and fitted to the wings of the line. This value for  $N_1$  would correspond to ionization of all hydrogen atoms initially in the tube. This experimental profile cannot be fitted by a theoretical profile for a single density; it is too broad in the wings and too narrow in the center. This probably indicates that the light originated in regions of different ion densities. This is just what one would expect, as the monochromator was looking through the ionizing front and through any "expansion fan" that might exist behind the front, regions characterized by gradients in the ion density. Considering the good agreement of the experimental data taken at 50  $\mu\text{sec}$  and later with the theoretical profiles, it seems reasonable to conclude that during the decay period the plasma is on the average homogeneous.

The largest source of error in determining the ion density from the experimental profiles is in the freedom of choice of a theoretical profile to fit the experimental data. Figure 6 shows the same experimental profile of  $H_\beta$  as seen in Fig. 3 but fitted this time with several theoretical profiles for comparison purposes. The solid lines show theoretical profiles for densities of 4.0, 5.0, and  $6.0 \times 10^{15} \text{ cm}^{-3}$ , all calculated for a temperature of  $10,000^\circ\text{K}$ . The best fit, assuming this temperature, is seen to be for  $N_1 = 5.0 \times 10^{15} \text{ cm}^{-3}$ . All the theoretical curves in this figure are drawn to coincide at their maximum values (at  $\Delta\lambda \approx 1.5 \text{ A}$ ). The same curves have also been redrawn, normalized to keep the total intensity constant (not shown in this figure), possibly a fairer comparison with the experimental data, but the conclusions are the same. Judging from Fig. 6, one might reasonably assign an error of about



MU-22965

Fig. 5. H $\beta$  profile 19  $\mu$ sec after the discharge was initiated. The profile is too narrow in the center and too broad in the wings to be fitted by a theoretical profile if a uniform ion density is assumed. The solid curve is a profile computed for  $N_i = 6.4 \times 10^{15}$  cm $^{-3}$ ,  $T = 10^4$  K, and fitted to the wings of the line.



MU-21657

Fig. 6.  $H_{\beta}$  profile, same as in Fig. 3, but showing several theoretical profiles for comparison purposes.

$\pm 0.5 \times 10^{15} \text{ cm}^{-3}$  in determining the ion density from this particular profile, owing to the freedom in choosing a theoretical curve at a given temperature to fit the experimental data.

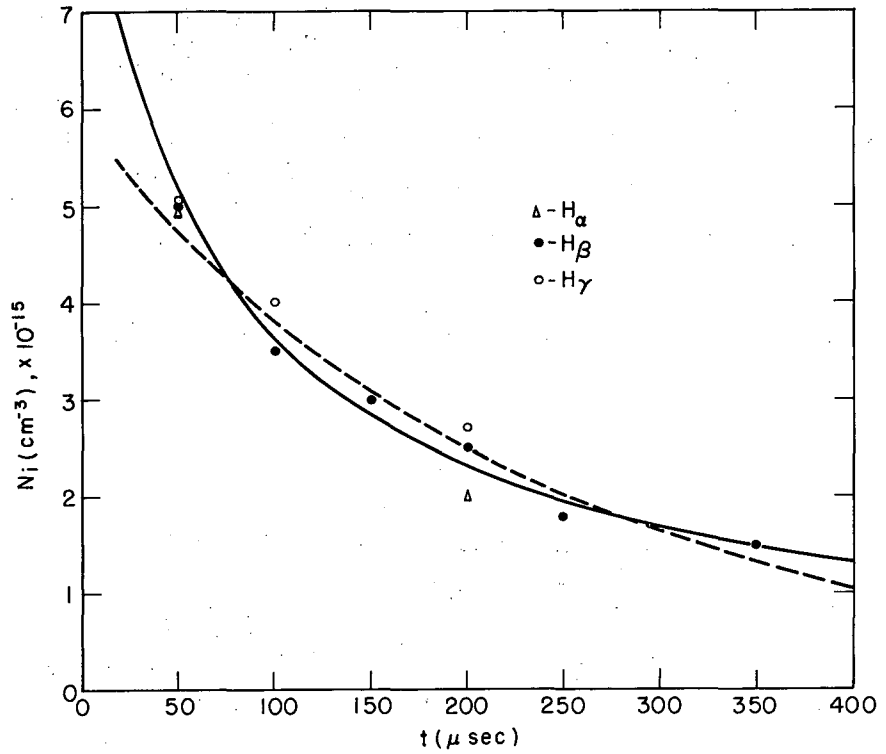
As stated previously, because of electron collision effects the shape of the theoretical curves is temperature-dependent. This temperature dependence is also shown in Fig. 6 for the case of the  $H_{\beta}$  profile. The dashed lines and the extended solid line on the left indicate theoretical profiles calculated for a constant ion density of  $5.0 \times 10^{15} \text{ cm}^{-3}$  and for three different temperatures, 5000, 10,000, and 20,000  $^{\circ}\text{K}$ . Fortunately the effect of varying the temperature over even this considerable range is slight. We see that varying the temperature assumed in calculating the theoretical profile by a factor of two is roughly equivalent to a 10% change in the estimated ion density. The temperature at 50  $\mu\text{sec}$  has been estimated to be about 12,000  $^{\circ}\text{K}$  by observing the ohmic damping of Alfvén waves; the damping is related to the electron temperature through the conductivity. Direct measurements of the electrical conductivity indicate about the same temperature. The ion temperature should equal the electron temperature at this time, as current ceased to flow through the plasma some 15  $\mu\text{sec}$  earlier, and electron-ion energy equipartition times (the time for ions and electrons to reach equilibrium with each other--see Spitzer<sup>11</sup>) are only a few hundredths of a  $\mu\text{sec}$ . Electron-electron energy distribution relaxation times are even shorter than this, so it is fair to assign a common temperature to both the ions and electrons at this time in the life of the plasma. There is some evidence also from the observed attenuation of Alfvén waves that the temperature after 50  $\mu\text{sec}$  does not fall very fast, and may be of the order of 6,000  $^{\circ}\text{K}$  at 150  $\mu\text{sec}$ . On this basis, and for simplicity, a temperature of 10,000  $^{\circ}\text{K}$  was assumed in fitting the theoretical profiles. Until more accurate temperature measurements have been made as a function of time, however, this source of error must remain in the ion density measurements.

On the basis of the above discussion of the sources of error affecting each ion density determination from an observed line profile, one might assign a reasonable error in each ion density measurement of  $\pm 0.7 \times 10^{15} \text{ cm}^{-3}$  for measurements early in the decay period, increasing to about  $\pm 1 \times 10^{15} \text{ cm}^{-3}$  for measurements late in time. The late measurements are more difficult because both the intensity and the width of the lines have decreased.

#### THE TIME DEPENDENCE OF THE ION DENSITY

Figure 7 shows the experimentally determined ion density as a function of time, using data from all three lines,  $H_{\alpha}$ ,  $H_{\beta}$ , and  $H_{\gamma}$ . Density measurements were made 50  $\mu\text{sec}$  after the discharge was initiated and later. Before this time the light intensity changes rapidly, making density determinations difficult. The density is observed to decay from  $5.0 \times 10^{15} \text{ cm}^{-3}$  at 50  $\mu\text{sec}$  (31  $\mu\text{sec}$  after crowbar) to about  $1.5 \times 10^{15} \text{ cm}^{-3}$  at 350  $\mu\text{sec}$  (331  $\mu\text{sec}$  after crowbar).

Two curves have been fitted to these data as an aid to extrapolating to times earlier than 50  $\mu\text{sec}$ . The solid line is a least-squares best fit, assuming the plasma decays according to the equation



MU-22430

Fig. 7. The observed time dependence of the ion density. Errors (not shown) in the experimental points are estimated to be  $\pm 0.7 \times 10^{15} \text{ cm}^{-3}$  early in the decay period, increasing to about  $\pm 1.0 \times 10^{15} \text{ cm}^{-3}$  late in the decay period. The solid line is a least-squares fit, if the decay rate is assumed to be proportional to the square of the ion density. The dashed line, also a least-squares fit, is based on assumption of an exponential decay.

$$\frac{dN_i}{dt} = -\alpha N_i^2$$

and assuming a constant  $\alpha$ . If the plasma were to decay by radiative recombination at constant temperature--two very questionable assumptions--the decay rate would be given by this equation. The fit is good and gives an  $\alpha$  of  $1.6 \times 10^{-12} \text{ cm}^3 \text{ sec}^{-1}$ . This curve extrapolates to an ion density of  $7.1 \times 10^{15} \text{ cm}^{-3}$  at the time of crowbar (19  $\mu\text{sec}$ ). If all the hydrogen initially in the tube were completely dissociated and ionized, and if there were no sources or sinks present, the ion density would be  $6.4 \times 10^{15} \text{ cm}^{-3}$ . This extrapolated value of  $7.1 \times 10^{15} \text{ cm}^{-3}$  should be taken to mean, then, that the plasma was 100% ionized at the time of crowbar, within the experimental errors.

The dashed curve is a least-squares best fit assuming an exponential decay,

$$\frac{dN_i}{dt} = -AN_i,$$

and fits the experimental data about as well as the solid curve; both curves are entirely within the estimated experimental errors in the data. The value of  $A$  determined this way is  $4.35 \times 10^3 \text{ sec}^{-1}$ . This curve, which would be characteristic of decay by the lowest mode of ambipolar diffusion, extrapolates to an ion density of  $5.5 \times 10^{15} \text{ cm}^{-3}$  at the time of crowbar, which would correspond to 86% ionization of the hydrogen initially in the tube.

The conclusions we are able to draw from the ion density decay curve shown in Fig. 7 are the following:

1. At the time the Alfvén wave measurements are usually made, about 35  $\mu\text{sec}$  after the discharge is initiated, the plasma is still very highly ionized. The ion density is greater than  $5 \times 10^{15} \text{ cm}^{-3}$ , which corresponds to more than 80% ionization of the atomic hydrogen initially in the tube. The fraction ionized may be as high as 100%.
2. The plasma decays rather slowly, with an e-folding time of about 200  $\mu\text{sec}$ .
3. It is impossible to identify the means by which the plasma decays by the shape of the decay curve.

#### INDEPENDENT SEMIQUANTITATIVE ION DENSITY MEASUREMENT

Use of the Inglis-Teller formula provided a quick semiquantitative check of our ion density measurements. If one examines the broadening of the individual lines of a series such as the Balmer series, one finds that the higher members of the series are broadened more than the lower members.

As the higher members of the series are also closer together than the lower members, one eventually reaches a point where the broadening of the lines is comparable to the spacing between them, and at this point the lines in the series blur together and are no longer visible as distinct lines. This is obvious in the spectrum as a depression of the series limit, and is equivalent to saying that the perturbation of the energy levels due to the Stark effect becomes comparable to the energy difference between two adjacent levels. By equating these two energy terms one can solve for the principal quantum number  $n_m$  of the upper level of the last distinct line of the series. This leads to the Inglis-Teller formula for  $n_m$  (for details of the deviation, see Unsöld,<sup>12</sup> or the original paper by Inglis and Teller<sup>13</sup>):

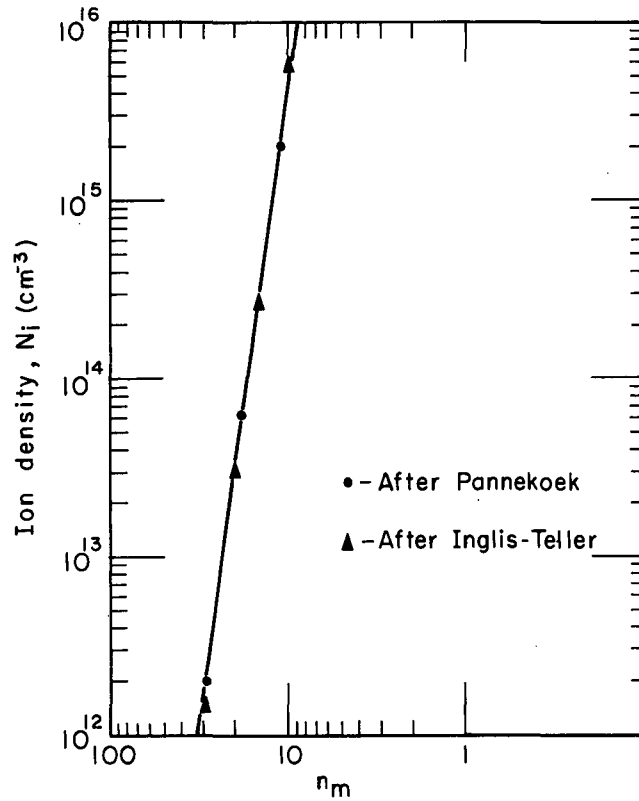
$$\log_{10} N_i = 23.26 - 7.5 \log_{10} n_m$$

Use of this formula to determine the ion density is equivalent to assuming the Holtzmark theory of line broadening, an assumption which the work of Griem, Kolb and Shen and others shows to be not well justified. In particular, this formula neglects the effects of electron collisions, which are not negligible at our temperatures and densities. Because of this the ion density as determined from the Inglis-Teller formula may be expected to be accurate at most to within a factor of 2.

A. Pannekoek in 1938 actually calculated the intensity distribution in the Balmer series near the series limit,<sup>14</sup> again using Holtzmark's theory of line broadening, the best available at the time. From his results one can estimate the number of lines that would be visible on a photographic plate. His results and those of Inglis and Teller are shown in Fig. 8, in which  $N_i$ , the ion density, is plotted against  $n_m$ , the principal quantum number of the highest distinct energy level. As the ground state of the transitions in the Balmer series is the  $n = 2$  state,  $n_m$  equals the number of lines visible in the Balmer spectrum plus 2. The results of the Inglis-Teller formula agree very well with the more accurate estimates made from Pannekoek's calculations.

In order to use these ideas to estimate the ion density in our hydrogen plasma we look at Fig. 9, which shows a spectrum of the discharge taken with a small Hilger-Watts spectrograph with quartz optics. The spectrum shows the entire Balmer series, beginning with  $H_\alpha$  on the left and extending well into the ultraviolet, showing the recombination continuum on the right. We distinctly see eight lines, and possibly nine. This gives  $n_m = 10$  or 11, and from Fig. 8 we see that this corresponds to  $N_i = 2 \times 10^{15}$  to  $4 \times 10^{15} \text{ cm}^{-3}$ , probably in better agreement with the ion density measurements as determined from the shapes of the profiles of the individual lines than we had any right to expect. The spectrographic plate integrates over time, so that this value of  $N_i$  is a mean value weighted by the intensity of the light as a function of the ion density.

Figure 10 shows the time dependence of the total  $H_\beta$  intensity integrated over a slit width of 50 Å and averaged over six shots. The times for  $N_i = 4 \times 10^{15} \text{ cm}^{-3}$  and  $2 \times 10^{15} \text{ cm}^{-3}$  are indicated, and it is apparent that



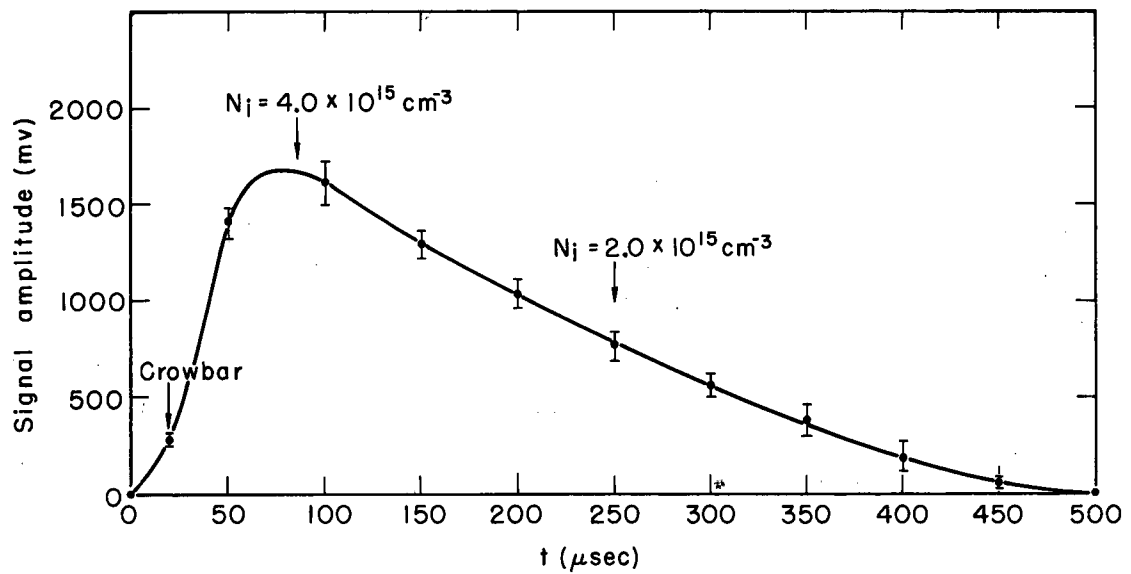
MU - 22431

Fig. 8. Ion density  $N_i$  vs principal quantum number  $n_m$  of the highest distinct quantum level. Here  $n_m$  equals the number of lines distinctly visible in the Balmer spectrum plus 2.



ZN-2735

Fig. 9. Spectrum of the discharge, showing the entire Balmer series, beginning with  $H_{\alpha}$  on the left and extending through the recombination continuum on the right. Note the very few faint but sharp impurity lines and the obvious Stark broadening of the Balmer lines. Eight or possibly nine lines are distinctly visible in the Balmer series.



MU-22432

Fig. 10. Total H $\beta$  intensity vs time. Slit width was 50 A.

most of the light did leave the plasma between these two times, consistent with the ion density estimates from the depression of the Balmer series limit shown in Fig. 9.

It should be pointed out that these two methods of determining the ion density--from the depression of the Balmer series limit and from the shape of the individual line profiles--are not fundamentally different, as both depend on the Stark broadening of the spectral lines. They are only different applications of the same effect.

If Alfvén waves are induced in the plasma soon after crowbar, when the ion density is still high, good agreement (within the experimental errors of a few per cent) is obtained<sup>3,4</sup> between the observed Alfvén wave velocity and the theoretical value based on the spectroscopically determined value for the ion density at that time that such an agreement is obtained. This may be taken as an additional independent confirmation of the accuracy of the ion-density measurements.

#### DECAY OF THE PLASMA

We shall now indulge in some speculation as to the mechanism by which the plasma decays. The most likely possibilities are by diffusion losses, by motion of the plasma to the walls due to instabilities or turbulence, or by volume recombination. Let us consider these various possibilities.

We can estimate the diffusion loss rate across the magnetic field. We treat the plasma as a conducting fluid, and estimate the time required for the plasma to drift across the magnetic field a distance comparable to the radius of the tube. Spitzer<sup>11</sup> gives, for the drift velocity (in cm sec<sup>-1</sup>) of a plasma across a strong magnetic field,

$$\vec{v}_{\perp} = - \frac{\eta}{B^2} \nabla p,$$

where  $\eta$  is the electrical resistivity in emu,  $B$  is the magnetic field strength in gauss, and  $p$  is the plasma pressure.

Assuming a temperature of 10,000 °K, the time required for an ion to undergo a 90 deg scattering "collision" is, from expressions given in Spitzer, about  $5 \times 10^{-10}$  sec. The ion cyclotron period with a magnetic field of 16,000 gauss is much longer, about  $4 \times 10^{-8}$  sec. The ions, then, in effect do not see the magnetic field, as they undergo many collisions in one ion cyclotron period. The electrons, however, undergo only a few collisions during one electron cyclotron period. We use for the electrical resistivity,  $\eta$ , the resistivity transverse to a strong magnetic field. This gives a somewhat higher value for  $\vec{v}_{\perp}$  (i. e., a more pessimistic loss rate) than the case in which the electrons make many collisions during one electron cyclotron period. The drift velocity then becomes

$$v_{\perp} = - \frac{\eta}{B^2} \nabla p = - \frac{1.29 \times 10^{13} z \ln \Lambda}{B^2 T^{3/2}} \nabla p \text{ cm sec}^{-1}.$$

For  $\nabla p$  we use  $\nabla(N_i kT) = kT \nabla N_i$ ; then we have

$$v_{\perp} = - \frac{1.78 \times 10^{-3} \ln \Lambda}{B^2 T^{1/2}} \nabla N_i.$$

If we assume  $T = 10^4 \text{ }^\circ\text{K}$ ,  $B = 16,000 \text{ gauss}$ ,  $\nabla N_i = - \text{ion density/radius of the tube} = -(5 \times 10^{15} \text{ cm}^{-3}) / 7 \text{ cm} = -0.7 \times 10^{15} \text{ cm}^{-4}$ , and  $\ln \Lambda = 6$ , then we have

$$v_{\perp} = 292 \text{ cm sec}^{-1}.$$

The time  $\tau$  required for the plasma to drift a distance equal to the radius of the tube is

$$\tau = \frac{R}{v_{\perp}} = \frac{7 \text{ cm}}{292 \text{ cm sec}^{-1}} = 24 \text{ msec.}$$

This estimate of the characteristic radial diffusion time, about 20 msec, is larger by two orders of magnitude than the observed characteristic decay time of 200  $\mu\text{sec}$ , so that it appears unlikely that radial diffusion losses dominate the decay of the plasma.

In this calculation of diffusion losses across the magnetic field we have neglected the effect of neutrals, certain to be present in the decaying plasma. However, in the model used in this calculation the loss rate is determined by the macroscopic electrical properties of the plasma, i. e., by the electrical resistivity. Since the electron-ion collision frequency (which, loosely speaking, determines the electrical resistivity) is larger by about two orders of magnitude than the electron-neutral collision frequency under the conditions assumed, the presence of neutrals should not greatly alter the estimated decay time.

The loss of plasma due to diffusion of the plasma along the magnetic field to the ends of the tube is harder to estimate. The loss is by ambipolar diffusion, which is determined by the rate of diffusion of ions. We assume that the ions recombine at the end plates, then diffuse back into the body of the plasma. The diffusion rate is then determined by charge-exchange collisions between ions and neutrals. The diffusion is governed by

$$\frac{\partial N_i}{\partial t} = D_a \nabla^2 N_i,$$

and the characteristics decay time  $\tau \approx L^2/D_a$ , where  $D_a$  is the ambipolar diffusion coefficient (just twice the ion diffusion coefficient if the ion and electron temperatures are equal), and  $L$  is a characteristic dimension of the plasma. From simple gas kinetic theory we have

$$D_a = 2D = 2 \frac{\bar{v}}{3N_n \sigma},$$

where  $\bar{v}$  is the mean thermal velocity of the ions,  $N_n$  is the neutral atomic hydrogen density, and  $\sigma$  is the charge-exchange collision cross section.

Taking the characteristic dimension,  $L$  to be 40 cm (about half the tube length), and assuming  $N_n = 2.0 \times 10^{15} \text{ cm}^{-3}$ ,  $\sigma = 6 \times 10^{15} \text{ cm}^2$ , (see footnote 7, Reference 3), and  $\bar{v} = 1.6 \times 10^6 \text{ cm sec}^{-1}$  (the mean thermal velocity of  $\text{H}^+$  ions at 10,000  $^\circ\text{K}$ ), we find

$$\tau = L^2/D_a = 18 \text{ msec},$$

again much longer than the observed decay time. These estimates of characteristic times for diffusion losses are the results of gross oversimplifications of the theory, but they are probably not off by two orders of magnitude.

We have no evidence of loss of the plasma in the decay period by cooperative phenomena such as turbulence or instabilities. The power input into the plasma during the decay period is essentially zero, precluding any type of driven instability. Also, the plasma pressure is very low compared with the magnetic field pressure;  $\beta$ , the ratio of the two, is about  $10^{-3}$  ( $\beta < 1$  is a necessary but not sufficient condition for stability). The light from the central region of the plasma--the total  $\text{H}_\beta$  line intensity, for example--decays smoothly with time, and does not indicate any violent motion of the plasma into or out of the region observed by the monochromator. High-frequency turbulence in the plasma, which might lead to "enhanced diffusion," also seems unlikely in the decay period; probe measurements indicate that the time rate of change of the azimuthal magnetic field in the plasma at this time is only a few gauss/ $\mu\text{sec}$ .

We conclude, then, that because of the strong axial magnetic field and the considerable length of the plasma, the rates of diffusion losses in the radial and longitudinal directions, respectively, are less by about two orders of magnitude than the observed decay rate of the plasma. Loss of the plasma to the walls by instabilities or turbulence seems unlikely. Therefore the plasma probably decays by a volume recombination process.

The most probably volume recombination processes that may take place in a plasma consisting of hydrogen ions and electrons are radiative recombination, corresponding to the reaction  $\text{H}^+ + e^- \rightarrow \text{H} + h\nu$ , and three body recombination, the third body being an electron. This type of recombination corresponds to  $\text{H}^+ + e^- + e^- \rightarrow \text{H} + e^-$ , with the second electron

carrying off the excess kinetic energy. Dissociative recombination depends on the presence of molecular ions, which should not be present at a temperature of  $10,000^\circ\text{K}$ .

In calculating radiative recombination coefficients, the assumption is usually made that the energy levels of the excited atom are populated only by radiative capture of electrons to the level in question and by radiative transitions from higher levels. Zanstra has computed the radiative recombination coefficient  $\alpha$  as a function of temperature for hydrogen, using these assumptions.<sup>15</sup> His results are shown in Fig. 11, where we show the theoretical radiative recombination coefficient  $\alpha$  vs temperature. The recombination rate is then given by

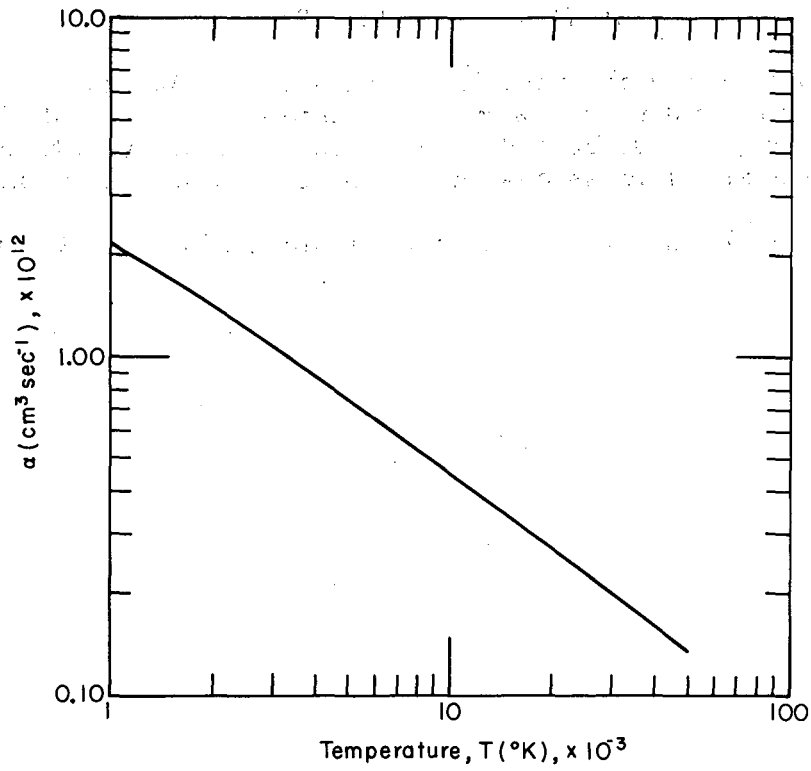
$$\frac{dN_i}{dt} = - \alpha(T) N_i^2.$$

Referring to the ion density decay curve shown in Fig. 7, and considering the errors in determining the ion density, we find that the observed decay rate may be explained by a recombination coefficient  $\alpha$  of  $1 \times 10^{-12}$  to  $2 \times 10^{-12} \text{ cm}^3 \text{ sec}^{-1}$ . From Fig. 11 we see that at a temperature of  $10^4 \text{ }^\circ\text{K}$  the predicted value of  $\alpha$  is  $0.45 \times 10^{-12} \text{ cm}^3 \text{ sec}^{-1}$ . Thus the observed decay rate is of the correct order of magnitude to be explained by radiative recombination.

A better approach to the problem is to consider in detail the means by which the various quantum states of the atom are populated and depopulated, solve for the distribution among the excited states, and from this calculate the rate of population of the ground state by radiative transitions, this then being the definition of the recombination event. This has been done by D'Angelo at Princeton for ion densities in the range  $10^{12}$  to  $10^{13} \text{ cm}^{-3}$  and temperatures of 1000 to  $10,000 \text{ }^\circ\text{K}$ .<sup>16</sup> He finds that the higher quantum levels are populated primarily by three-body recombination (the rate is proportional to the sixth power of the principal quantum number!) and depopulated both by ionizing electron collisions and by radiative transitions to lower levels. One must consider all the recombination processes to all the various levels to really treat the problem properly at these ion densities. If the recombination rate is again proportional to the square of the ion density, the coefficient now has to be a function of both the temperature and the density,

$$\frac{dN_i}{dt} = - \alpha(N_i, T) N_i^2.$$

In general, higher recombination rates are predicted than with the assumption of only radiative recombination. Using ionization and recombination rates derived in a paper by Elwert<sup>17</sup> and repeating D'Angelo's calculations for a temperature of  $10^4 \text{ }^\circ\text{K}$  and an ion density of  $1 \times 10^{15}$  to  $6.4 \times 10^{15} \text{ cm}^{-3}$ , we find an  $\alpha$  of  $1.5 \times 10^{-12}$  to  $2.7 \times 10^{-12} \text{ cm}^3 \text{ sec}^{-1}$ , in good agreement with the observed  $\alpha$  of  $1 \times 10^{-12}$  to  $2 \times 10^{-12} \text{ cm}^3 \text{ sec}^{-1}$ .



MU-21664

Fig. 11. Radiative radiation coefficient  $\alpha$  vs temperature, after Zanstra.

It must be pointed out that any recombination process is temperature-dependent, sometimes quite strongly so, and until more accurate temperature measurements have been made, any close agreement between observed and theoretical recombination rates may be largely fortuitous. For the same reason, the shape of the ion-density decay curve is temperature-dependent, although the relatively large errors in measuring the ion density may obscure this detail.

#### ACKNOWLEDGMENTS

The authors wish to thank Dr. C. M. Van Atta and William R. Baker for their interest in this work. We also thank Dr. Wulf B. Kunkel, Dr. Klaus Halbach, Dr. Robert V. Pyle, and Dr. John M. Stone for many helpful comments and discussions during the course of the work.

This work was done under the auspices of the U. S. Atomic Energy Commission.

## REFERENCES

1. T. K. Allen, W. R. Baker, R. V. Pyle, and J. M. Wilcox, *Phys. Rev. Letters* 2, 383 (1959).
2. J. M. Wilcox, F. I. Boley, and A. W. DeSilva, *Phys. Fluids* 3, 15 (1960).
3. John M. Wilcox, Alan W. DeSilva, William S. Cooper III, and Forrest I. Boley, Experiments on Alfvén-Wave Propagation (UCRL-9482, Nov. 1960) in *Proceedings, Lockheed Symposium on Magnetohydrodynamics*, Dec. 16-17, 1960.
4. A. W. DeSilva, W. S. Cooper III, and J. M. Wilcox, Alfvén Wave Reflections and Propagation Modes UCRL-9496, Feb. 1961.
5. J. Holtsmark, *Ann. Physik* 58, 577 (1919).
6. H. R. Griem, A. C. Kolb, and K. Y. Shen, *Phys. Rev.* 116, 4 (1959); *idem.* NRL Report 5455 (1960).
7. P. Bogen, *Z. Physik* 149, 62 (1957).
8. B. Mozer, Tech. Report No. 3, Contract NONR-760 (15), Carnegie Institute of Technology, 1960.
9. H. Margenau and M. Lewis, *Revs. Modern Phys.* 31, 569 (1959).
10. R. D. Cowan and G. H. Dieke, *Revs. Modern Phys.* 20, 418 (1948).
11. Lyman Spitzer, *The Physics of Fully Ionized Gases* (Interscience Publishers, Inc., New York, 1956).
12. A. Unsöld, *Physik der Sternatmosphären* (Springer-Verlag, Berlin, 1955), p. 325.
13. D. R. Inglis and E. Teller, *Astrophys. J.* 90, 439 (1939).
14. A. Pannekoek, *Monthly Notices, Royal Astronomical Society* 98, 694 (1938).
15. H. Zanstra, *Proc. Roy. Soc. (London)* A186, 236 (1946).
16. N. D'Angelo, Recombination of Ions and Electrons (USAEC Report MATT-15, 1960); *Phys. Rev.* 121, 505 (1961).
17. G. Elwert, *Z. Naturforsch* 7a, 432 (1952).

This report was prepared as an account of Government sponsored work. Neither the United States, nor the Commission, nor any person acting on behalf of the Commission:

- A. Makes any warranty or representation, expressed or implied, with respect to the accuracy, completeness, or usefulness of the information contained in this report, or that the use of any information, apparatus, method, or process disclosed in this report may not infringe privately owned rights; or
- B. Assumes any liabilities with respect to the use of, or for damages resulting from the use of any information, apparatus, method, or process disclosed in this report.

As used in the above, "person acting on behalf of the Commission" includes any employee or contractor of the Commission, or employee of such contractor, to the extent that such employee or contractor of the Commission, or employee of such contractor prepares, disseminates, or provides access to, any information pursuant to his employment or contract with the Commission, or his employment with such contractor.

